JOURNAL OF SPACECRAFT AND ROCKETS
Vol. 43, No. 5, September–October 2006

Trajectories for Human Missions to Mars, Part 2: Low-Thrust Transfers

Damon F. Landau* and James M. Longuski†
Purdue University, West Lafayette, Indiana, 47907-2023

DOI: 10.2514/1.21954

We compute optimal low-thrust transfers (with constant thrust and constant specific impulse) between Earth and Mars over a range of flight times (from 120 to 270 days) and launch years (between 2009 and 2022). Unlike impulsive transfers, the mass-optimal trajectory depends strongly on the thrust and specific impulse of the propulsion system. A low-thrust version of the rocket equation is provided where the initial mass or thrust may be minimized by varying the initial acceleration and specific impulse for a given power-system specific mass and for a trajectory time of flight. With fixed time-of-flight transfers there is a minimum thrust and a maximum allowable specific mass; that is, if the available thrust is too low or the specific mass is too large then the desired transfer does not exist. We find the minimum allowable thrust for constrained time-of-flight missions is on the order of a few Newtons per metric ton of payload for power systems with tens of kg/kW. As expected, the thrust and ΔV requirements of the trajectories decrease with increasing flight times. By extending the flight time from 180 to 270 days the ΔV is reduced by 40% for powered captures and up to 35% for aeroassisted capture trajectories.

Nomenclature

a_0	=	initial acceleration due to thrust, m/s^2
f_t	=	tankage factor, %
g	=	standard acceleration due to gravity at Earth's surface, 9.80665 m/s^2
I_{sp}	=	specific impulse, s
m_{pay}	=	payload, mt
m_0	=	initial mass, mt
$\dot{m}$	=	mass flow rate, kg/s
P	=	power, kW
T	=	thrust, N
t_b	=	burn time, s
α	=	specific mass, kg/kW
η	=	efficiency, %

I. Introduction

THE concept of traveling to Mars in a low-thrust vehicle has been explored since the 1950s [1–8]. Moreover, there have been several decades of low-thrust trajectory optimization to support the design of human missions to Mars [9–21]. The most popular use of low thrust in Mars missions is for cargo transfer, where time insensitive payloads can take years to reach Mars from Earth. However, these transfers are not suitable for crew transport because the long flight times expose the crew to excessive radiation and to microgravity and often entail short stay times at Mars. [We do not examine cargo transfers in this paper as they have been sufficiently treated in the literature (see, for example, [10,17]).] To fairly compare low-thrust missions with impulsive ones, the interplanetary time of flight (TOF) and the Mars stay time for the crew transfer vehicle should be the same. For example, a low-thrust mission with 1 yr transfers and a 1 yr stay time puts the crew at more risk for less return than a high-thrust mission with half-year transfers and 1.5 years on Mars. We compute optimal low-thrust trajectories with TOF from 120 to 270 days (the same TOF constraints as the impulsive transfers in Part 1) so the mission timelines with low thrust are consistent with the impulsive transfer missions. Results are provided for both powered capture and aeroassisted trajectories. Because Earth–Mars trajectory characteristics approximately repeat every seven synodic periods (14.95 years), we examine trajectories over a span of seven missions (with launch dates from 2009–2022).

Received 26 July 2005; accepted for publication 21 December 2005.

*Doctoral Candidate, School of Aeronautics and Astronautics, 315 N. Grant St.; landau@ecn.purdue.edu. Student Member AIAA.

†Professor, School of Aeronautics and Astronautics, 315 N. Grant St.; longuski@ecn.purdue.edu. Associate Fellow AIAA.

II. Trajectory Models

Low-thrust trajectory legs are modeled as a series of constrained ΔVs, which mimics the effect of continuous low-magnitude acceleration [18]. Primer vector analysis [22] is not required in our low-thrust optimizer as the number of (constrained) impulses is set a priori, and the steering history is a direct optimization vector. We compute direct (Earth–Mars and Mars–Earth) low-thrust trajectories for both powered and aeroassisted arrivals with the objective of maximizing the final mass of the spacecraft. The initial spacecraft state is the position and velocity of the departure planet. The target planet's position and velocity are matched for powered arrivals (thus $V_\infty = 0$), but only the position is matched for aeroassisted arrivals (where $V_\infty \neq 0$). The planetocentric portion of the trajectory is assumed to be fixed (i.e., we assume the spacecraft is launched optimally off the surface to reach $V_\infty = 0$), though better performance is possible when both the planetocentric and heliocentric portions are optimized as a whole trajectory [19]. These low-thrust trajectories do not necessarily minimize mission cost, but are indicative of the type of trajectory that would optimize a human mission to Mars.

We use a sequential quadratic programming algorithm [23] to compute minimum-ΔV trajectories with bounded TOF. (By bounded we mean the TOF may be less than or equal to the constrained value. Moreover, the departure and arrival dates can vary freely as long as the TOF between them is within the bound.) The low-thrust optimization problem is more complex than the impulsive optimization problem. The low-thrust transfers are constructed with 50 constrained ΔVs, which results in 160 design variables (50ΔV plus the time, V_∞, and spacecraft mass at Earth and Mars), 57 nonlinear inequalities (50ΔV magnitudes plus the position, velocity, and mass at a match point), 3 linear equalities ($V_\infty = 0$ and fixed departure mass), and 1 linear inequality (TOF).

On the other hand, the optimization problem for direct impulsive trajectories can require as few as two design variables (Earth and Mars encounter times) and one linear inequality (bounded TOF). The more challenging impulsive cycler optimization problem has 73

variables (25 planetary encounter times plus the position and time of 12 deep space maneuvers), 23 nonlinear equalities (flyby $V_\infty = 0$), 23 nonlinear inequalities (flyby altitudes), and eight linear inequalities (TOF). Impulsive trajectories are calculated in MATLAB and the low-thrust transfers are calculated using FORTRAN with software that was previously developed at Purdue. (We found that due to the size of the low-thrust problem our MATLAB code rarely converges for low-thrust transfers, while the FORTRAN code almost always converges in a timely manner.)

For each trajectory type, we initially optimized the long TOF (270-day) trajectory for the 2009 outbound opportunity. The 270-day TOF trajectory served as the initial guess for the 260-day TOF trajectory, and so on (by 10-day intervals) until the 120-day TOF transfer was optimized. The whole process was then repeated for the subsequent synodic periods up to the 2022 outbound opportunity.

III. Results

Determining the maximum payload for a low-thrust transfer requires optimization of the propulsion system along with the trajectory. For example, an increase in thrust lowers the ΔV (and the propellant mass fraction) for the vehicle, but the hardware mass must increase to provide additional power to the thrusters. Consequently, there is a trade between low propellant mass with high power levels and low hardware mass at low power levels. The balance in this trade is usually determined by the specific mass (α) and efficiency (η) of the propulsion system. The specific mass determines the ratio between the hardware (power source, thrusters, etc.) and the amount of power it produces

$$\alpha \equiv m_{\text{hardware}}/P_{\text{electric}} \tag{1}$$

and the efficiency is the ratio of jet power to hardware power

$$\eta \equiv P_{\text{jet}}/P_{\text{electric}} \tag{2}$$

The jet power may be determined from

$$P_{\text{jet}} = TgI_{\text{sp}}/2 \tag{3}$$

Thus, the hardware mass is

$$m_{\text{hardware}} = \alpha TgI_{\text{sp}}/(2\eta) \tag{4}$$

and, for constant α and η, increases proportionally with the thrust and specific impulse. The propellant tanks also contribute a significant portion of the spacecraft mass, and the tank mass may be estimated via the tankage factor

$$f_t \equiv m_{\text{tank}}/m_{\text{propellant}} \tag{5}$$

The final-to-initial mass fraction may be computed for low-thrust missions via the rocket equation [24]

$$\Delta V = \int_0^{t_b} a\,dt = \int_0^{t_b} \frac{T}{m}\,dt = \int_0^{t_b} \frac{\dot{m}gI_{\text{sp}}}{m}\,dt = \int_{m_0}^{m_f} \frac{gI_{\text{sp}}}{m}\,dm$$
$$= gI_{\text{sp}}\,\ell_n\left(\frac{m_0}{m_f}\right) \tag{6}$$

The mass ratio may be written explicitly as

$$\frac{m_0}{m_f} = e^{\Delta V/gI_{\text{sp}}} \tag{7}$$

where we assume that the thrust and specific impulse are constant and that the thrust may be computed by

$$T = \dot{m}gI_{\text{sp}} \tag{8}$$

The rocket equation is particularly useful in determining the ratio of initial mass (payload, hardware, tankage, and propellant) to payload mass

$$\frac{m_0}{m_{\text{pay}}} = \frac{e^{\Delta V/gI_{\text{sp}}}}{1 - e^{\Delta V/gI_{\text{sp}}}(\alpha/2\eta)a_0 gI_{\text{sp}} - f_t(e^{\Delta V/gI_{\text{sp}}} - 1)} \tag{9}$$

Thus, the spacecraft thrust is (the constant value):

$$\frac{T}{m_{\text{pay}}} = \frac{a_0 e^{\Delta V/gI_{\text{sp}}}}{1 - e^{\Delta V/gI_{\text{sp}}}(\alpha/2\eta)a_0 gI_{\text{sp}} - f_t(e^{\Delta V/gI_{\text{sp}}} - 1)} \tag{10}$$

Unlike impulsive trajectories, the ΔV for low-thrust transfers depends on the acceleration and specific impulse of the spacecraft [i.e., $\Delta V = \Delta V(a_0, I_{\text{sp}}, \text{TOF})$]. From Eqs. (4) and (10) the hardware mass also depends on acceleration and specific impulse. As a result, the initial mass [Eq. (9)] for low-thrust trajectories is minimized when the ΔV is balanced against the hardware mass—both of which depend on the variables a_0 and I_{sp}. The optimization problem is thus to minimize $m_0/m_{\text{pay}}[a_0, I_{\text{sp}}, \Delta V(a_0, I_{\text{sp}}, \text{TOF}), \alpha/\eta, f_t]$ by varying a_0 and I_{sp} with constant TOF, α/η, and f_t. We note that the trajectory optimization problem (minimize ΔV for constant a_0, I_{sp}, and TOF subject to $a \le T/m$) is a subset of the mass optimization problem (in our formulation).

Therefore, to minimize the initial mass [Eq. (9)] or to minimize the thrust [Eq. (10)], an accurate means of determining the minimum ΔV for a given trajectory TOF and vehicle a_0 and I_{sp} is required. (In our ΔV minimization problem we assume free departure and arrival dates and optimum thrust vector history subject to TOF and acceleration constraints.) Zola [11] describes an approximate analytic method to calculate ΔV as a function of a_0 and I_{sp}, provided the ΔV-optimal burn time t_b for a trajectory with the same TOF is known. In contrast to the maximum-acceleration trajectories provided in Part 1, we present the ΔV for a direct transfer from Earth to Mars (and vice versa) using the minimum possible acceleration during launch years 2009–2022 in Fig. 1. In the specific case of Fig. 1 we calculated trajectories that match the heliocentric orbit of Mars from the orbit of Earth and set the mass flow rate to zero (corresponding to an infinite I_{sp}). Because the acceleration is minimized, the burn time for these trajectories is equal to the TOF (i.e., the thruster is always on). Using this data, we found that Zola's heuristic method produces values for optimum payload mass fractions to within a few percent (say, 3%). Alternatively, numerical optimization techniques provide higher fidelity results at the expense of longer computation time. Example low-thrust trajectories are presented in Fig. 2. For completeness the stay time and mission duration for the trajectories in Fig. 1 are provided in Fig. 3.

Let us consider a 210-day Earth-to-Mars transfer in 2014 with a transfer vehicle mass (payload) of 40 mt, an electric propulsion system with $\alpha/\eta = 30$ kg/kW, and a tankage factor of 5%. The lowest possible thrust for this transfer is 110 N with $a_0 = 0.712$ mm/s^2, $I_{\text{sp}} = 2,050$ s, and $\Delta V = 14.3$ km/s. (We note that the minimum acceleration at $I_{\text{sp}} = 2,050$ s is 0.639 mm/s^2 with $\Delta V = 17.3$ km/s.) The required thrust is usually on the order of a few Newtons per metric ton of payload for constrained TOF missions, but the exact value depends on the assumed hardware

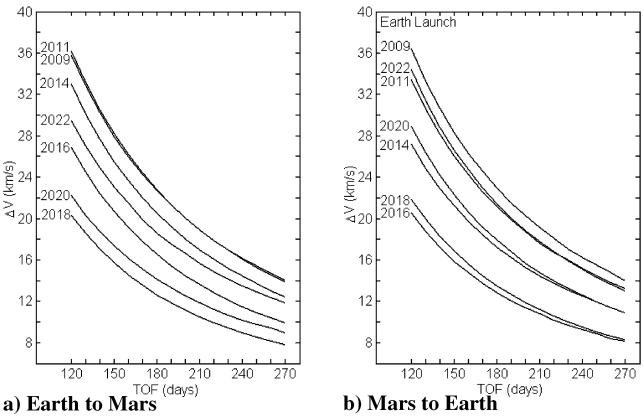

a) Earth to Mars **b) Mars to Earth**

Fig. 1 ΔV for minimum-acceleration transfers with powered capture.

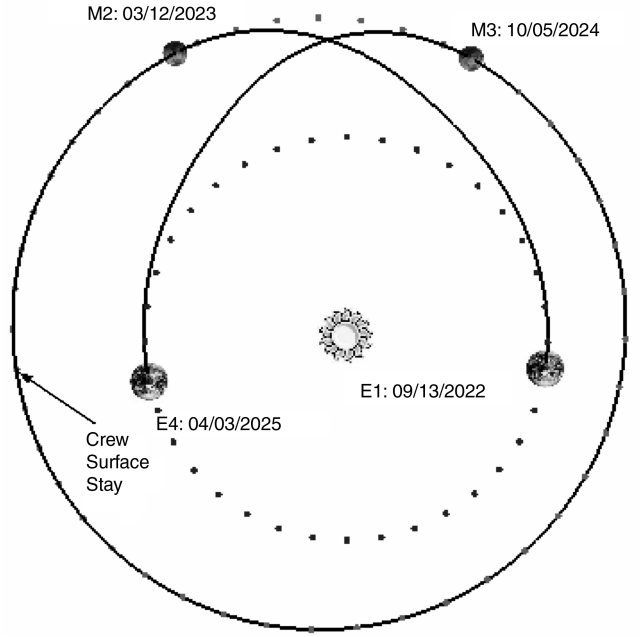

Fig. 2 Low-thrust transfers with $V_\infty = 0$ at each planetary encounter.

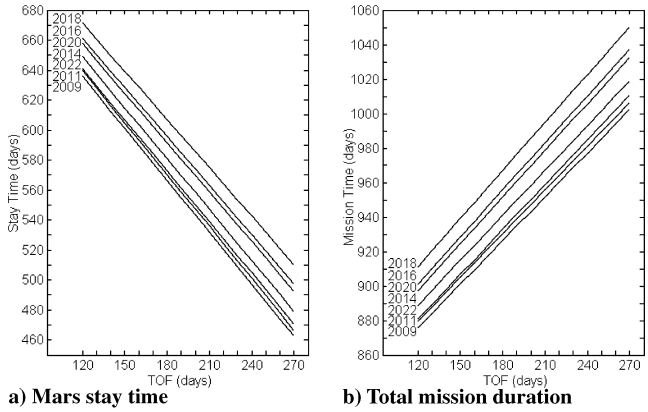

a) Mars stay time **b) Total mission duration**

Fig. 3 Stay time and mission duration for powered capture low-thrust transfers.

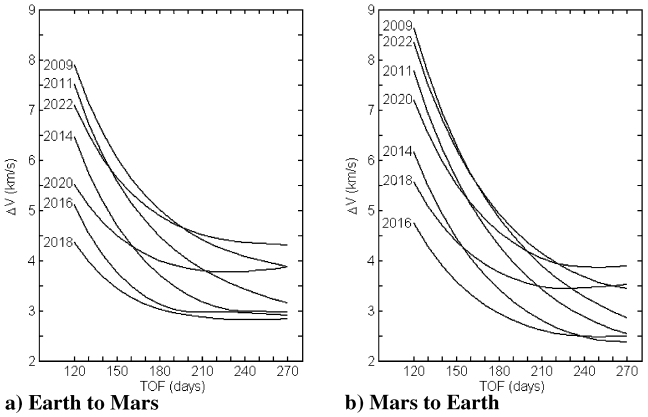

a) Earth to Mars **b) Mars to Earth**

Fig. 4 ΔV for low-thrust transfers with aerocapture or direct entry.

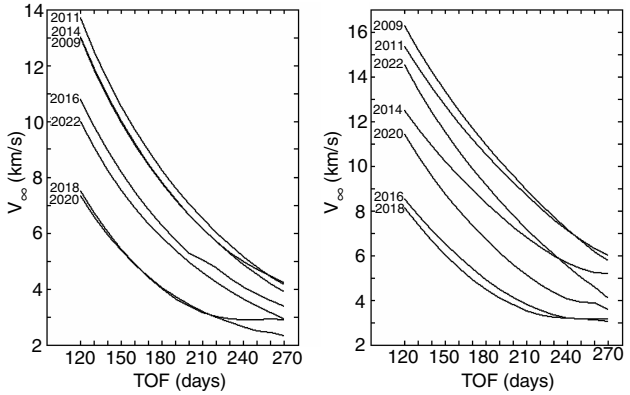

a) Earth to mars **b) Mars to earth**

Fig. 5 Arrival V_∞ for low-thrust transfers with aerocapture or direct entry.

development (i.e., α/η). In addition to a minimum thrust limit, there is also a maximum allowable α/η for low-thrust missions [when the denominator of Eq. (9) approaches zero]. For example, transfers with TOF around 120 days are enabled only when $\alpha/\eta < 20$ kg/kW (with $I_{sp} > 1,000$ s) and regular (i.e., at every launch opportunity) 120-day transits do not exist unless $\alpha/\eta < 10$ kg/kW.

We also examined minimum-acceleration transfers for aerocapture missions (for arrival $V_\infty \neq 0$) but found that the V_∞ at arrival was impractical (i.e., it is often at least double the impulsive transfer V_∞). Instead, we optimized low-thrust trajectories with infinite I_{sp} (i.e., assuming constant mass) and set the acceleration to the levels found in Fig. 1 for a given launch year and TOF combination. The resulting ΔV and arrival V_∞ (where the launch V_∞ is zero) are found in Figs. 4 and 5, respectively. Because the same initial acceleration was used to calculate the powered and aeroassisted capture trajectories, the burn time is given by $t_b = (\Delta V_A/\Delta V_P)$ TOF where ΔV_P is the powered arrival ΔV (from Fig. 1) and ΔV_A is the aeroarrival ΔV (from Fig. 4). We note that increasing the acceleration decreases the ΔV and burn time, and in the limit of infinite thrust and zero burn time (corresponding to impulsive ΔV), the ΔV approaches the sum of the departure and arrival V_∞ for powered capture missions and becomes the departure V_∞ for aeroassisted capture.

Let us again consider a 210-day transit in 2014 with 40 mt of payload, 8 mt for the heat shield (at arrival), $\alpha/\eta = 30$ kg/kW, and $f_t = 5\%$. Instead of minimizing the thrust (which would result in excessive arrival V_∞), we set the acceleration to the same value as the powered-arrival example, $a_0 = 0.712$ mm/s^2. In this case, an I_{sp} of 2,050 s results in a thrust level of 54 N with a ΔV of 3.2 km/s (again using Zola's method) and 6.4 km/s arrival V_∞ (as in Fig. 5). We find that the required thrust levels for aeroassisted transfers with moderate V_∞ are usually around one Newton per metric ton of payload. However, for low-thrust mission optimization we recommend including a constraint to limit the arrival V_∞, or as a rule of thumb, setting the acceleration to at least the same level as that of a powered-arrival trajectory. The hardware limits for aeroassisted trajectories are less stringent than those for powered-arrival transfers as the α/η can be as large as 50 kg/kW for the most demanding 120-day transfers.

While the trajectory characteristics shown in Figs. 1–5 and the vehicle properties given by Eqs. (9) and (10) are produced assuming constant thrust and I_{sp} (as in nuclear electric propulsion), the results also apply (indirectly) to trajectories with variable thrust and I_{sp} (as in solar electric propulsion). Unlike the constant power of nuclear electric propulsion, the power available from a solar electric propulsion system drops off with the inverse square of the distance from the sun. Thus, the power available at Earth is double the power available at Mars. As a result, either the thrust or I_{sp} (or both) must be lower at Mars than at Earth [from Eq. (3)]. Even though the thrust and I_{sp} may vary during an Earth–Mars transfer, minimum-ΔV trajectories with bounded TOF have similar characteristics (e.g., the same ΔV and V_∞ to within a few percent) as long as the average acceleration and I_{sp} are the same. Thus the average acceleration and specific impulse (over the burn time) may be substituted into constant thrust and constant I_{sp} models to determine the ΔV, V_∞, thrust, and mass fractions of solar electric systems.

For example, consider the minimum-acceleration transfers in Fig. 1. The ΔV for these trajectories do not vary significantly with

different thrust profiles. While a solar electric system produces more thrust (and more acceleration) near Earth and less near Mars than a nuclear electric system (with constant thrust) the total ΔV for a given TOF is very nearly the same for both systems. Because the ΔV and burn time (t_b = TOF) are the same, the average acceleration $a_{ave} = \Delta V/t_b$ is also the same. Therefore, for solar electric propulsion trajectories with powered capture, the spacecraft must provide more acceleration and I_{sp} near Earth and less acceleration and I_{sp} near Mars than a nuclear electric system to produce the same (optimal) ΔV. Again, as long as the average acceleration and I_{sp} are the same, the trajectory ΔV will be nearly equal (even for transfers above the minimum acceleration limit).

This property (of comparable ΔV and V_∞ when the average acceleration and I_{sp} are the same) also applies to trajectories with aeroassisted capture. We designed trajectories with a solar electric propulsion system so that the average acceleration and I_{sp} are the same as the trajectories in Fig. 4 and found that the ΔV and arrival V_∞ agreed to within 3%. For aeroassisted trajectories, the thrusting occurs near Earth for Earth–Mars transfers and near Mars for Mars–Earth transfers. Thus, the available power (from the solar panels) does not vary as much for aeroassisted captures as for powered captures, which require thrusting near both Earth and Mars. Moreover, the actual acceleration more closely matches the average acceleration for aeroassisted trajectories, which makes it easier to estimate an initial acceleration to size the thrust level of the solar electric system. For powered arrivals, the initial acceleration is significantly higher (for Earth departures) or lower (for Mars departures) than the average acceleration, which makes it more difficult to estimate the necessary thrust levels over the trajectory. We note that for any type of electric propulsion system there is a minimum required thrust to achieve a given TOF and a maximum allowable α/η to provide margin for payload in the final spacecraft mass.

A notable difference between the impulsive-ΔV curves (in Part 1) and the minimum-acceleration curves (Fig. 1) is that the impulsive transfers typically flatten out by 270-day TOF (i.e., a local minimum exists below a TOF of 270 days) whereas the minimum-thrust ΔV continue to decrease at 270-day TOF. The aeroassisted low-thrust curves (Fig. 4) do not exhibit the same behavior because the acceleration was set to a specific value (determined from Fig. 1) for each launch year and TOF combination. Indeed, there is a range of optimal ΔV values for a given launch opportunity and maximum TOF as the thrust varies from a minimum value to infinity (i.e., impulsive thrusting). The trajectories in Figs. 1–5 are designed to limit the acceleration requirements of an electric propulsion system to the lowest practical values for the crew transfer vehicles. (Of course, lower acceleration and longer TOF would be appropriate for cargo transfers.)

Further, the low-thrust curves do not rise as sharply as the impulsive-ΔV curves at low TOF. In Fig. 1 the ΔV doubles from 270- to 150-day TOF (similar to most impulsive transfers), but the 120-day TOF ΔV is only about 2.6 times the 270-day TOF ΔV across each launch opportunity (the corresponding impulsive-ΔV ratio is significantly higher). The relative ΔV reduction from 180-day TOF to 270-day TOF for minimum-acceleration trajectories is about 40%, while the relative reduction from 180 days to 210 days is closer to 17% across all launch opportunities. The ΔV for aeroassisted capture trajectories increase at a less uniform rate over the different launch opportunities. For example, the ΔV ratio from a TOF of 270 days to 120 days is only about 1.5 when Mars is near perihelion (during 2016–2018), but the same ratio is approximately 2.4 (for Earth–Mars transfers) and 3.0 (for Mars–Earth transfers) when Mars is at aphelion (during 2009–2011). The impulsive aeroassisted direct trajectories exhibit a relatively steeper rise from 270- to 120-day TOF, yet retain the same disparity between trajectories when Mars is at perihelion or aphelion. There is also a broad range in the reduction in ΔV from 180-day TOF to 270-day TOF aeroassisted trajectories. When Mars is near perihelion the reduction is only about 5% (for the given acceleration levels), but the ΔV is reduced by up to 30% for outbound transfers and 40% for the inbound trajectories when Mars is near aphelion. The mass savings that may be gained by extending the allowable TOF depends mainly on the vehicle mass and I_{sp}, but a TOF extension of only one or two months can lead to a considerable reduction in mission mass.

From Fig. 3 we note that the stay time decreases linearly and the mission time increases linearly as a function of TOF for low-thrust missions. (Though not shown, the stay time and mission duration of aeroassisted trajectories are usually three weeks shorter than the powered capture times found in Fig. 3.) The impulsive curves (direct transfers in Part 1) exhibit similar trends at lower TOF, but begin to flatten out by about 200 days TOF. The difference occurs because most impulsive trajectories reach a local minimum for ΔV at TOF below 270 days while low-thrust trajectories continue to lose ΔV as the TOF is extended beyond 270 days. (Unlike impulsive trajectories, low-thrust transfers are not significantly affected by the complications of a plane change around 180° transfer angles.) The mission duration for impulsive and low-thrust transfers are about the same at low TOF, but the duration for low-thrust missions is about 2 months longer (out of 2.6 years) at longer flight times. Compared with impulsive missions, the stay time for low-thrust transfers varies over the TOF range, but is usually within 1 month (out of 1.5 years) of the impulsive stay time. For preliminary trade studies, the Mars stay time and total mission duration are approximately the same for low-thrust and impulsive transfers with constrained TOF. A summary of low-thrust versus impulsive transfers is provided in Table 1.

IV. Conclusions

We investigate low-thrust trajectories with short transfers (TOF from 120 to 270 days) that are suitable for crew transport. Seven missions with launch dates from 2009–2022 are examined to cover an entire 15-year Earth–Mars synodic cycle. As with impulsive transfers, the ΔV is lower when Mars is near perihelion (2016 and 2018 launch years) and the ΔV is higher when Mars is near aphelion (during the 2009 and 2022 missions). The ΔV for aeroassisted capture trajectories is significantly lower than the ΔV for powered captures, but the aeroassisted arrival V_∞ tend to become higher with low-thrust transfers than with impulsive trajectories. Further reductions in ΔV are available by extending the TOF beyond the NASA-recommended 180 days. By increasing the TOF by 1 month to 210 days the ΔV decreases by 17%, (by 7.5 km/s). Further if we choose 270-day transfers over 180-day transfers, up to 39%, or 17.5 km/s, of ΔV is eliminated from the mission.

Because the acceleration and specific impulse directly affect the minimum ΔV for a low-thrust transfer, we recommend optimizing the trajectory and the electric propulsion system simultaneously. The specific mass-to-efficiency ratio α/η of the propulsion system provides an efficient means to balance the propellant mass against the hardware mass while minimizing the initial mass or required thrust for a given payload and TOF. From a trajectory standpoint, the

Table 1 Qualitative comparison of low-thrust and impulsive trajectories[a]

Characteristic	Low-thrust	Impulsive
Burn time	Weeks	Minutes
Total ΔV	Larger	Smaller
ΔV is function of	TOF, a_0, and I_{sp}	TOF
ΔV sensitivity to TOF and launch year	Less	More
Mission feasibility drivers	Thrust and α/η	Propellant mass fractions

[a]For similar flight time and mission duration.

primary benefit of increasing the TOF or employing aeroassisted capture is a reduction in ΔV; however, these trajectory choices also play an important role in the necessary hardware for a low-thrust vehicle. As the trajectory ΔV decreases, lower thrust levels are required and power systems with larger specific masses may be used to complete the transfer.

If people are to travel to Mars in low-thust vehicles, then judicious trajectory design will be required to tailor the propulsion systems with the available technology.

Acknowledgments

Damon F. Landau's work has been sponsored in part by a National Defense Science and Engineering Graduate (NDSEG) Fellowship and a National Science Foundation Graduate Research Fellowship.

References

[1] Stuhlinger, E., "Electrical Propulsion System for Space Ships with Nuclear Power Source," *Journal of the Astronautical Sciences*, Part 1, Vol. 2, winter 1955, pp. 149–152; Part 2, Vol. 3, spring 1956, pp. 11–14; Part 3, Vol. 3, summer 1956, p. 33.

[2] Irving, J. H., and Blum, E. K., *Comparative Performance of Ballistic and Low-Thrust Vehicle for Flight to Mars*, Vol. 2, Vistas in Astronautics, Pergamon Press, Oxford, England, U.K., 1959, pp. 191–218.

[3] King, J. C., Shelton, R. D., Stuhlinger, E., and Woodcock, G. R., "Study of a Nerva-Electric Manned Mars Vehicle," *AIAA/American Astronomical Society Stepping Stones to Mars Meeting*, AIAA, New York, 1966, pp. 288–301.

[4] Braun, R. D., and Blersch, D. J., "Propulsive Options for a Manned Mars Transportation System," *Journal of Spacecraft and Rockets*, Vol. 28, No. 1, 1991, pp. 85–92.

[5] Walberg, G., "How Shall We Go to Mars? A Review of Mission Scenarios," *Journal of Spacecraft and Rockets*, Vol. 30, No. 2, 1993, pp. 129–139.

[6] Niehoff, J. C., and Hoffman, S. J., *Pathways to Mars: An Overview of Flight Profiles and Staging Options for Mars Missions*, Science and Technology Series of the American Astronautical Society, Univelt, Inc., San Diego, CA, 1996, Vol. 86, pp. 99–125; also American Astronomical Society, Paper 95-478.

[7] Donahue, B. B., and Cupples, M. L., "Comparative Analysis of Current NASA Human Mars Mission Architectures," *Journal of Spacecraft and Rockets*, Vol. 38, No. 5, 2001, pp. 745–751.

[8] Landau, D. F., and Longuski, J. M., "Comparative Assessment of Human Missions to Mars," American Astronomical Society Paper 03-513, *American Astronomical Society/AIAA Astrodynamics Specialist Conference*, Univelt, Inc., San Diego, 2004.

[9] Moekel, W. E., "*Fast Interplanetary Missions with Low-Thrust Propulsion Systems*," NASA, Rept. TR-R-79, 1961.

[10] Melbourne, W. G., and Sauer, C. G., "Optimum Interplanetary Rendezvous with Power-Limited Vehicles," *AIAA Journal*, Vol. 1, No. 1, 1963, pp. 54–60.

[11] Zola, C. L., "*A Method for Approximating Propellant Requirements of Low-Thrust Trajectories*," NASA, Rept. TN-D-3400, 1966.

[12] Ragsac, R. V., "Study of Electric Propulsion for Manned Mars Missions," *Journal of Spacecraft and Rockets*, Vol. 4, April 1967, pp. 462–468.

[13] Kawaguchi, J., Takiura, K., and Matsuo, H., "On the Optimization and Application of Electric Propulsion to Mars and Sample and Return Mission," American Astronomical Society/AIAA, Spaceflight Mechanics Meeting, Cocoa Beach, FL, 1994, American Astronomical Society Paper 94-183.

[14] Chang-Diaz, F. R., Hsu, M. M., Braden, E., Johnson, I., and Yang, T. F., "*Rapid Mars Transits with Exhaust Modulated Plasma Propulsion*," NASA, Rept. TP-3539, 1995.

[15] Tang, S., and Conway, B. A., "Optimization of Low-Thrust Interplanetary Trajectories Using Collocation and Nonlinear Programming," *Journal of Guidance, Control, and Dynamics*, Vol. 18, No. 3, 1995, pp. 599–604.

[16] Gefert, L. P., Hack, K. J., and Kerslake, T. W., "Options for the Human Exploration of Mars Using Solar Electric Propulsion," *STAIF, Proceedings of the Conferences on Applications of Thermophysics in Microgravity and on Next Generation Launch Systems, and 16th Symposium on Space Nuclear Power and Propulsion*, American Institute of Physics, Woodbury, NY, 1999, pp. 1275–1280.

[17] Williams, S. N., and Coverstone-Carrol, V., "Mars Missions Using Solar-Electric Propulsion," *Journal of Spacecraft and Rockets*, Vol. 37, No. 1, 2000, pp. 71–77.

[18] McConaghy, T. T., Debban, T. J., Petropoulus, A. E., and Longuski, J. M., "An Approach to Design and Optimization of Low-Thrust Trajectories with Gravity Assists," American Astronomical Society Paper 01-468, *American Astronomical Society/AIAA Astrodynamics Specialist Conference*, Univelt, Inc., San Diego, 2002.

[19] Whiffen, G. J., and Sims, J. A., "Application of the SDC Optimal Control Algorithm to Low-Thrust Escape and Capture Trajectory Optimization," American Astronomical Society Paper 02-208, *American Astronomical Society/AIAA Space Flight Mechanics Conference*, Univelt, Inc., San Diego, 2002.

[20] Sankaran, K., Cassady L., Kodys, A. D., and Choueiri, E. Y., "A Survey of Propulsion Options for Cargo and Piloted Missions to Mars," *Annals of the New York Academy of Sciences*, Vol. 1017, May 2004, pp. 450–467.

[21] Chen, K. J., McConaghy, T. T., Landau, D. F., Longuski, J. M., and Aldrin, B., "Powered Earth–Mars Cycler with Three Synodic-Period Repeat Time," *Journal of Spacecraft and Rockets*, Vol. 42, No. 5, 2005, pp. 921–927.

[22] Lawden, D. F., *Optimal Trajectories for Space Navigation*, Butterworths, London, U.K., 1963.

[23] Gill, P. E., Murray, W., and Saunders, M. A., "SNOPT: An SQP Algorithm for Large-Scale Constrained Optimization," *SIAM Journal on Optimization*, Vol. 12, No. 4, 2002, pp. 979–1006.

[24] Tsiolkovsky, K. E., "Exploration of the Universe with Reaction Machines," *Science Review*, St. Petersburg, Russia, Vol. 5, 1903.

C. Kluever
Associate Editor